Supporting Information

Rechargeable Zn-ion Batteries with High Power and Energy Density: a Two-Electron Reaction Pathway in Birnessite MnO_2 Cathode Materials

Guanzhou Li[1,2,#], *Zongxiong Huang*[1,2,#], *Jinbiao Chen*[1,2], *Fu Yao*[1,2], *Jianping Liu*[1,2],

Oi Lun Li[3] , *Shuhui Sun*[4,*] , *Zhicong Shi*[1,2,*],

[1] Smart Energy Research Centre, School of Materials and Energy, Guangdong University of Technology, Guangzhou, 510006, PR China

[2] Guangdong Engineering Technology Research Center for New Energy Materials and Devices, Guangzhou, 510006, PR China

[3] School of Materials Science and Engineering, Pusan National University, Busan, 46241, Korea

[4] Institut National de la Recherche Scientifique-Énergie Matériaux et Télécommunications, Varennes, Quebec J3X 1S2, Canada

*Corresponding authors: zhicong@gdut.edu.cn (Z. Shi), shuhui@emt.inrs.ca

[#] These authors contributed equally to this work.

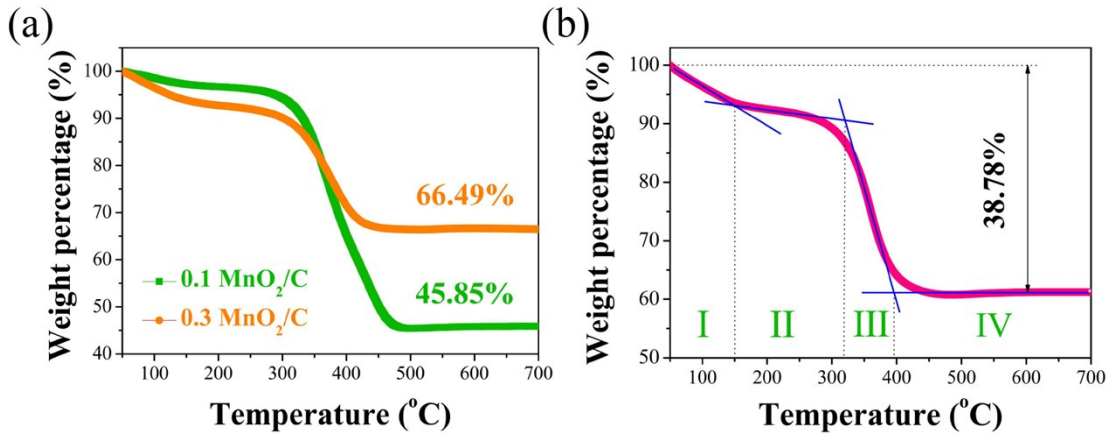

Figure S1. (a) TGA curves of 0.1 MnO_2/C and 0.3 MnO_2/C in the air. (b) The TGA curve (red line) of 0.2 MnO_2/C in the air and the blue line is the tangent of the red line.

According to the shape of the TGA curve, the material change process can be divided into four stages with the risen of temperature. The mass loss within 150 °C corresponds to the gasification of the adsorbed water on the material, and then the oblique platform situating between 150-320 °C is responsible for the loss of crystallization water in MnO_2. Following that, the subsequent stage of huge mass loss is caused by the intense combustion of Super P in the air. Ultimately, the last platform represents the remaining MnO_2.

Calculation of the molecular formula of MnO_2/C

The K/Mn (called as α) of MnO_2/C was obtained through the ICP-MS. In the meantime, the weight ratios of crystalline water (H_2O_{cry}), carbon and $K_\alpha MnO_2$ in composites, which were marked as β, γ and δ respectively, were tested by the thermogravimetric analysis. In addition, the H_2O_{cry}/Mn (ε) and C/Mn (η) are

calculated as follow:

$$\varepsilon = \frac{\beta}{M_{(H_2O)}} \div \frac{\delta}{M_{(K_\alpha MnO_2)}} = \frac{\beta \cdot M_{(K_\alpha MnO_2)}}{\delta \cdot M_{(H_2O)}} \quad (1)$$

$$\eta = \frac{\gamma}{M_{(C)}} \div \frac{\delta}{M_{(K_\alpha MnO_2)}} = \frac{\gamma \cdot M_{(K_\alpha MnO_2)}}{\delta \cdot M_{(C)}} \quad (2)$$

M(x) is the molar mass of substance X. Ultimately, the molecular formulas ($K_\alpha(H_2O)_\varepsilon MnO_2/C_\eta$) can be gained.

Table S1. The molecular formulas of different samples.

Sample	K:Mn (α)	H_2O_{cry}:Mn (ε)	C:Mn (η)	Molecular Formula
0.1 MnO_2/C	0.28	0.16	8.89	$K_{0.28}(H_2O)_{0.16}MnO_2/C_{8.89}$
0.2 MnO_2/C	0.34	0.24	4.01	$K_{0.34}(H_2O)_{0.24}MnO_2/C_{4.01}$
0.3 MnO_2/C	0.36	0.23	3.09	$K_{0.36}(H_2O)_{0.23}MnO_2/C_{3.09}$
calcined-MnO_2	0.32	0	0	$K_{0.32}MnO_2$

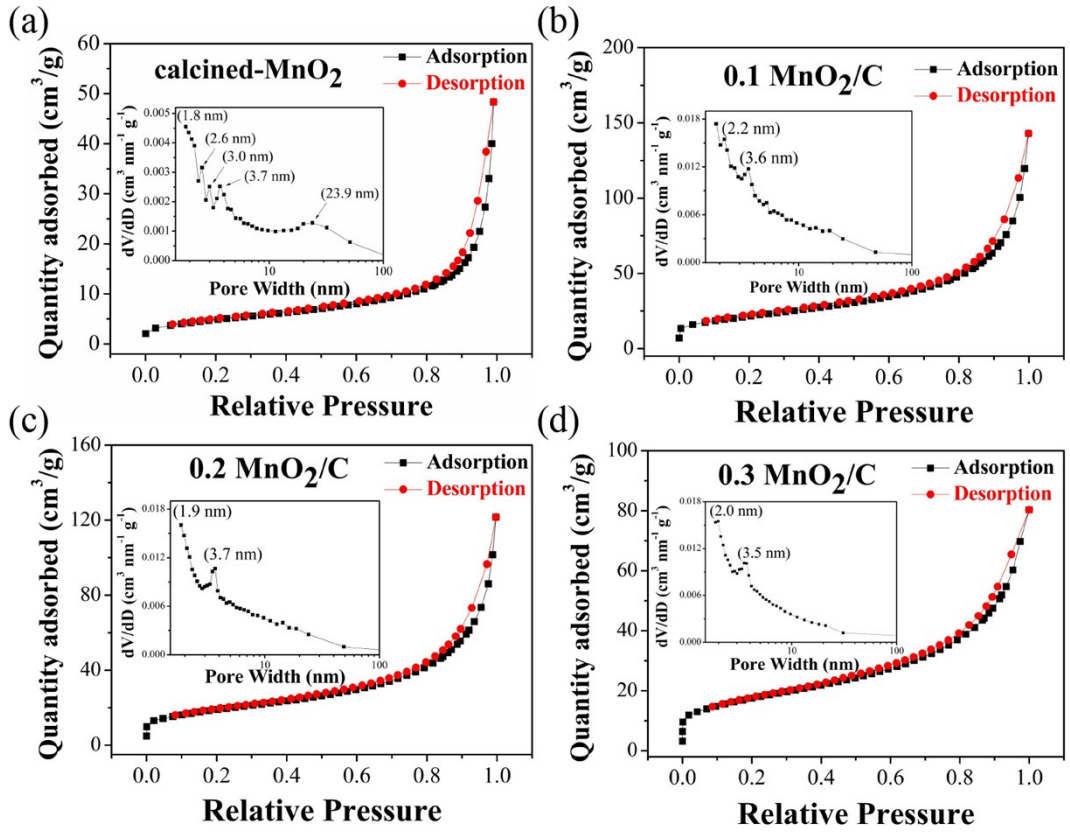

Figure S2. The N_2 adsorption/desorption isotherm of calcined-MnO_2 (a), 0.1 MnO_2/C (b), 0.2 MnO_2/C (c) and 0.3 MnO_2/C (d). The insets are the corresponding pore width distribution.

From Figure S2, it can be known that the N_2 adsorption-desorption isotherm curves of calcined-MnO_2 and MnO_2/C samples are belong to the IV isotherm curve, reflecting that the pore size of the materials are mainly located in the mesoporous range.[1] Meanwhile, the inset displays that calcined-MnO_2 and MnO_2/C samples are mainly with micropores and mesopores. Simultaneously, the pore size distribution of calcined-MnO_2 is broader and mainly distribute at 1.8 nm, 2.6 nm, 3.0 nm, 3.7 nm and 23.9 nm, while the main pore size distribution of 0.1 MnO_2/C (2.2 and 3.6 nm), 0.2 MnO_2/C (1.9 and 3.7 nm) and 0.3 MnO_2/C (2.0 and 3.5 nm) are narrower. The larger pore size of calcined-MnO_2 is mainly attributed to its large particle size and irregular

shape (Figure 2e and f). When the calcined-MnO_2 is piled up, it is easy to form a cavity between large particles and then some relatively larger holes are produced.

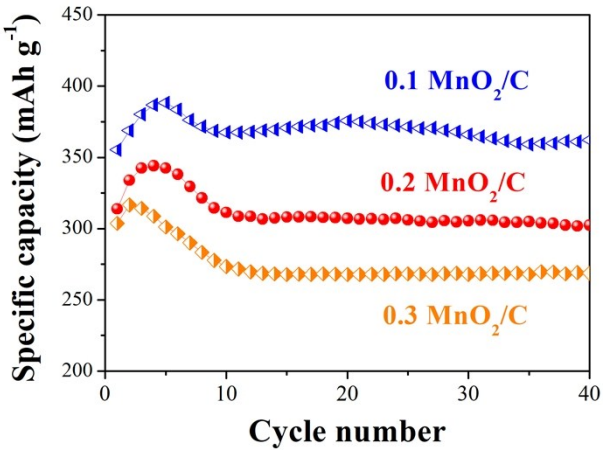

Figure S3. Cycling performance of 0.1 MnO_2/C-Zn battery, 0.2 MnO_2/C-Zn battery and 0.3 MnO_2/C-Zn battery at a current density of 300 mA g^{-1}.

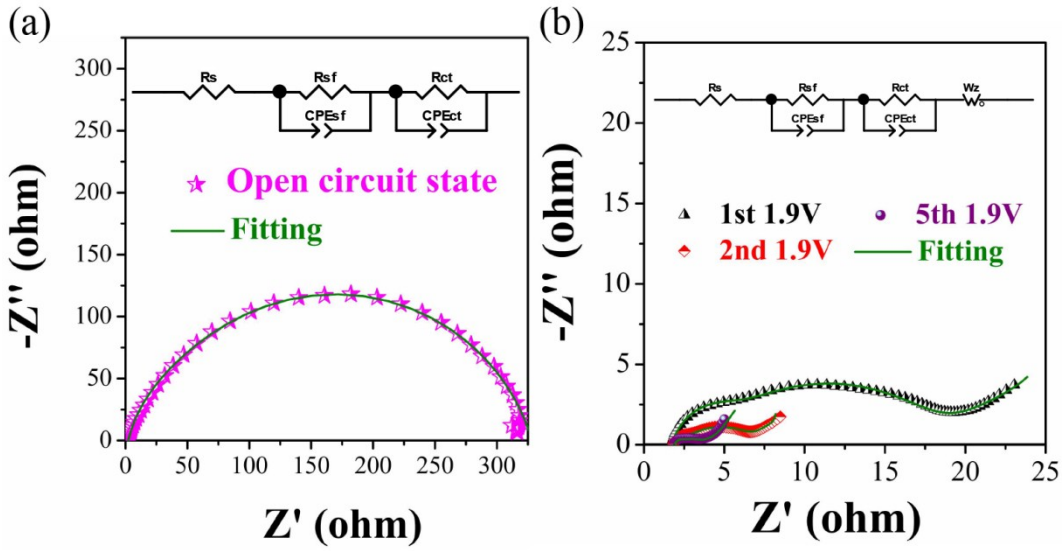

Figure S4. The Nyquist plots of 0.2 MnO_2/C electrode in coin cell at open circuit state (a) and 1.9V of different cycles (b) as well as the corresponding equivalent circuit model used to fit the experimental results.

Table S2. The R_s, R_{sf} and R_{ct} of the 0.2 MnO_2/C-Zn battery at different state corresponding to Figure S4.

Coin cell	R_s (Ω)	R_{sf} (Ω)	R_{ct} (Ω)
Open circuit state	1.74	310	16.3
1st 1.9V	1.63	2.61	13.6
2nd 1.9V	1.80	0.607	4.32
5th 1.9V	1.88	0.401	1.08

Table S3. The R_s, R_{sf} and R_{ct} of the Zn plate at different state as well as the polished Zn plate at open circuit state corresponding to Figure 3a-c.

Zn plate	R_s (Ω)	R_{sf} (Ω)	R_{ct} (Ω)
Open circuit state	1.43	250	95.0
1st discharge	1.27	6.19	4.30
2nd discharge	1.31	2.74	4.10
5th discharge	1.37	0.480	1.07
6th discharge	1.49	0.433	0.825
Polished Zn plate at open circuit state	2.50	11.6	3.03

Table S4. The R_s, R_{sf} and R_{ct} of the 0.2 MnO_2/C cathode at different state corresponding to Figure 3d.

Cathode	R_s (Ω)	R_{ct} (Ω)
Open circuit state	3.08	4.72
1st charge	2.88	4.60
2nd charge	2.79	2.27
5th charge	2.50	0.600
6th charge	2.48	0.598

Table S5. Discharge specific capacities of the 0.2 MnO_2/C-Zn battery at various current densities from 120 to 6000 mA g^{-1}.

Current Density (mA g^{-1})	120	300	600	1200	1800	2400	3000	3600	4200	4800	5400	6000
Specific Capacity (mAh g^{-1})	320	295	274	245	227	213	203	189	174	161	153	143

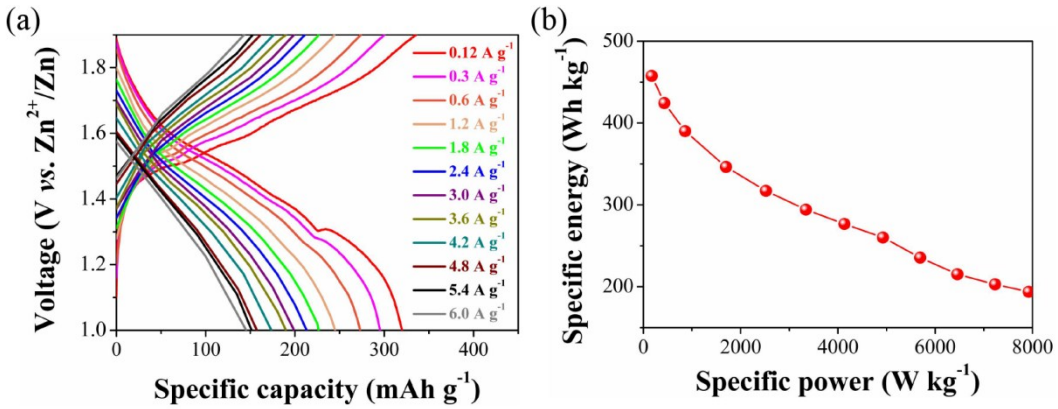

Figure S5. (a) Discharge-charge profile at various current densities corresponding to Figure 3a. (b) The Ragone plot of the 0.2 MnO_2/C-Zn battery. The Energy density and power density were calculated for the cathode only.

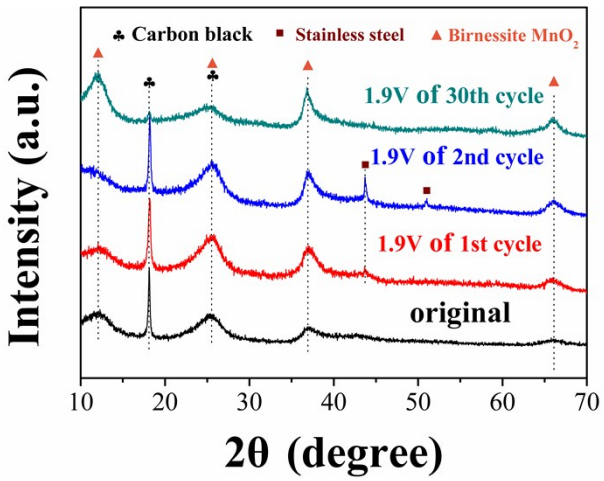

Figure S6. The XRD of 0.2 MnO_2/C cathode at original state and at 1.9 V of different cycles.

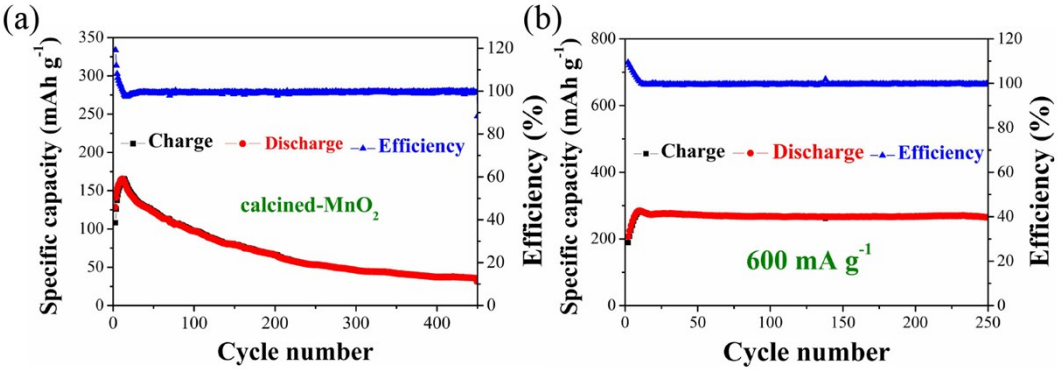

Figure S7. (a) Cycling performance of the calcined-MnO_2-Zn battery at a current density of 300 mA g^{-1}. (b) Cycling performance of the 0.2 MnO_2/C-Zn battery at a current of 600 mA g^{-1}.

Table S6. The K^+ and Mn^{2+} concentrations of electrolyte tested by ICP-MS in different states of the 0.2 MnO_2/C-Zn battery.

Sample	1.9V at 1st charge	1.0V at 1st discharge	1.9V at 2nd charge
Mn^{2+} (mol L^{-1})	0.50	2.26	1.39
K^+ (mmol L^{-1})	32.90	32.52	32.79

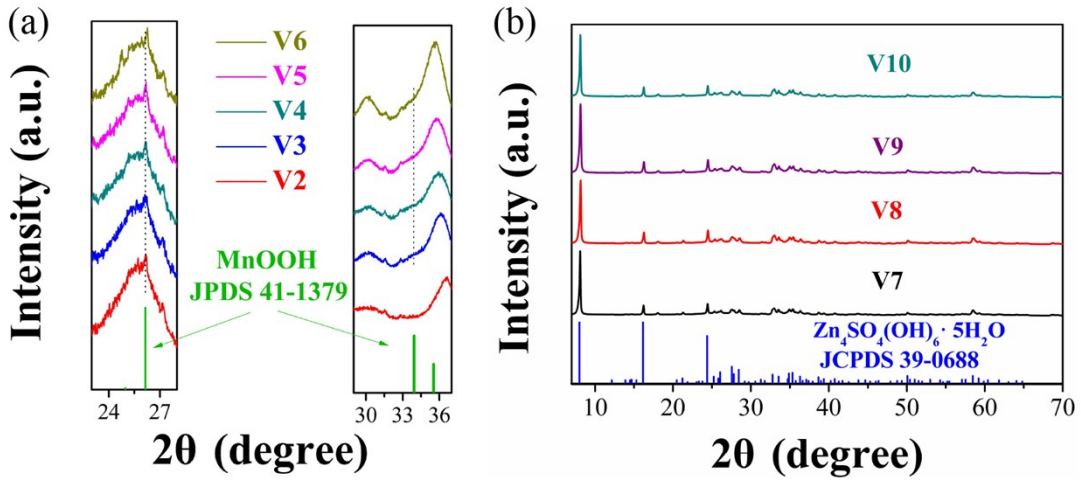

Figure S8. (a) The magnified XRD peaks of MnOOH in Figure 5b. (b) The XRD full patterns of Figure 5c.

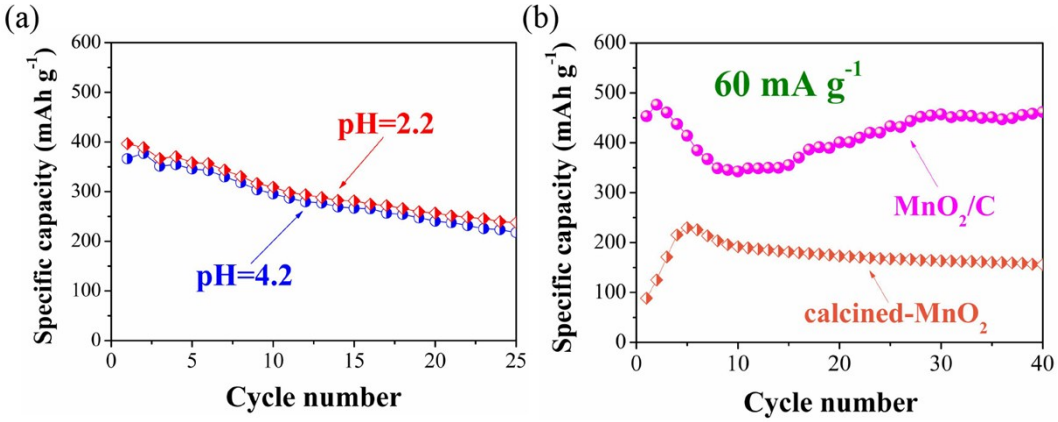

Figure S9. (a) Cycling performance of the 0.2 MnO_2/C-Zn battery in 2 M $ZnSO_4$+0.1 M $MnSO_4$ with different pH at a current density of 60mA g^{-1}. (b) Cycling performance of the 0.2 MnO_2/C-Zn battery and the calcined-MnO_2-Zn battery at a current density of 60 mA g^{-1}.

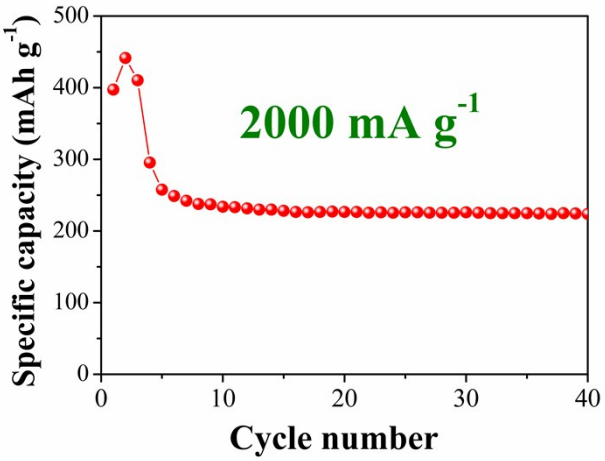

Figure S10. Cycling performance of the 0.2 MnO_2/C-Zn battery at a current density of 2000mA g^{-1}. The first three cycles belongs to the activation with 60 mA g^{-1}

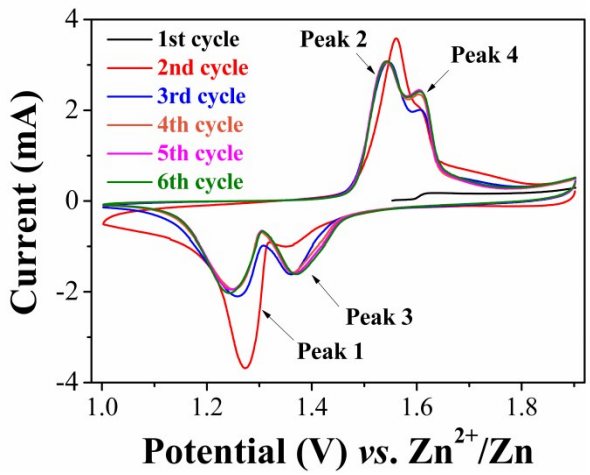

Figure S11. The CV performance of 0.2 MnO_2/C-Zn battery with 0.1M $MnSO_4$ at a scan rate of 0.1 mV s^{-1} in the potential window of 1.0-1.9 V *vs.* Zn^{2+} /Zn.

Table S7. The current ratio of Peak 1-Peak 4 at different scant rates corresponding to Figure 8c.

Scan Rate (mV s^{-1})	**0.1**	**0.2**	**0.4**	**0.6**	**0.8**	**1.0**	**1.2**	**2.4**
$I_{Peak\ 1}/I_{Peak\ 3}$	1.43	1.25	1.12	1.01	0.97	0.93	0.92	0.96
$I_{Peak\ 2}/I_{Peak\ 4}$	1.19	1.23	1.16	1.04	0.96	0.93	0.89	0.91

Table S8. The calculated parameters of the ion diffusion coefficient.

Voltage (V)	Active material	n	C_{ion} ($\times 10^4$ mol m^{-3})	σ	D_{ion} ($\times 10^{-13}$ cm^2 S^{-1})
1.63	$Zn_2Mn_4O_8 \cdot H_2O$	4	2.24	1.18	1.55
1.77	MnOOH	1	4.91	1.10	94.9

Table S9. Comparison the performances of the previously reported cathodes and MnO_2/C cathode in Zn-ion batteries.

Cathode material	**Electrolyte**	**Anode material**	**Capacity (mAh g^{-1})**	**Energy density (Wh kg^{-1})**	**Power density (W kg^{-1})**	**Cycling stability**	**Ref.**
Ca_2MnO_4	2 M $ZnSO_4$ + 0.1 M	Zinc foil	250 (100 mA	-	-	no abvious fluctuation in	2

	$MnSO_4$		g^{-1})			capacity after 1000 cycles (1 A g^{-1})	
$Mn_{0.15}V_2O_5 \cdot nH_2O$	1 M $Zn(ClO_4)_2$ in propylene carbonate	Zinc metal	367 (100 mA g^{-1})	225	375	42% capacity retention after 8000 cycles (10 A g^{-1})	3
Potassium vanadates	2 Ml $ZnSO_4$	Zinc metal	247 (300 mA g^{-1})	222.3	3600	100% capacity retention after 300 cycles (6 A g^{-1})	4
Molybdenum trioxide	poly(vinyl alcohol)(PVA)/$ZnCl_2$ gel	Zinc plate	241.3 (400 mA g^{-1})	14.4 (mWh cm^{-3})	9.79 (mW cm^{-3})	70.4% capacity retention after 400 cycles (6 A g^{-1})	5
$(NH_4)_2V_6O_{16} \cdot 1.5H_2O$	3 M Zn $(CF_3SO_3)_2$ aqueous electrolyte	Zinc foil	120 (100 mA g^{-1})	295.68	75.49	75% capacity retention after 10000 cycles (8 A g^{-1})	6
MnO_2@CNT film	$ZnSO_4$/$MnSO_4$/xanthan gel	Zn foil	260 (1C)	364	2500	90% capacity retention after 330 cycles (1C)	7
MnO_2@A4-type paper	1 M $ZnSO_4$ (pH4.0)	Zn foil	285 (0.05mA cm^{-2})	-	-	64% capacity retention over 40 cycles	8
MnO_2@PPy@ stainless steel	$ZnSO_4$/MnSO4/gelatin–borax gel	Deposited-Zn@nitinol wire	135.2 (1 C)	-	-	60% capacity retention after 1000 cycles	9
MnO_2@CNT yarn	$ZnSO_4$/$MnSO_4$/PAM gel	Deposited-Zn@CNT yarn	302.1	53.8 (mWh cm^{-3})	-	98.5% capacity retention after 500 cycles	10
MnO_2/C	2 M $ZnSO_4$ + 0.5 M $MnSO_4$	Zinc plate	295 (300 mA g^{-1})	260	4926	61.8% capacity retention after 1500 cycles (2 A g^{-1})	this work

NOTES AND REFERENCES

1 K. S. W. Sing, *Pure and applied chemistry*, 1982, **54**, 2201-2218.

2 S. Guo, S. Liang, B. Zhang, G. Fang, D. Ma and J. Zhou, *ACS nano*, 2019, **13**, 13456-13464.

3 H. Geng, M. Cheng, B. Wang, Y. Yang, Y. Zhang and C. Li, *Advanced Functional Materials*, 2019, **1907684**.

4 B. Tang, G. Fang, J. Zhou, L. Wang, Y. Lei, C. Wan, T. Lin, Y. Tang and S. Liang, *Nano Energy*, 2018, **51**, 579-587.

5 X. He, H. Zhang, X. Zhao, P. Zhang, M. Chen, Z. Zheng, Z. Han, T. Zhu, Y. Tong and X. Lu, *Advanced Science*, 2019, **6**, 1900151.

6 S. Chen, Y. Zhang, H. Geng, Y. Yang, X. Rui and C. Li, *Journal of Power Sources*, 2019, **441**, 227192.

7 S. Zhang, N. Yu, S. Zeng, S. Zhou, M. Chen, J. Di and Q. Li, *J. Mater. Chem. A*, 2018, **6**, 12237.

8 M. H. Alfaruqi, V. Mathew, J. Gim, S. Kim, J. Song, J. P. Baboo, S. H. Choi and J. Kim, *Chem. Mater.*, 2015, **27**, 3609.

9 Z. Wang, Z. Ruan, Z. Liu, Y. Wang, Z. Tang, H. Li, M. Zhu, T. F. Hung, J. Liu, Z. Shi and C. Zhi, *J. Mater. Chem. A*, 2018, **6**, 8549.

10 H. Li, Z. Liu, G. Liang, Y. Huang, Y. Huang, M. Zhu, Z. Pei, Q. Xue, Z. Tang, Y. Wang, B. Li and C. Zhi, *ACS Nano*, 2018, **12**, 3140.